"Active Flux" DTFC-SVM Sensorless Control of IPMSM

Ion Boldea, *Fellow, IEEE*, Mihaela Codruta Paicu, Gheorghe-Daniel Andreescu, *Senior Member, IEEE*, and Frede Blaabjerg, *Fellow, IEEE*

***Abstract*—This paper proposes an implementation of a motion-sensorless control system in wide speed range based on "active flux" observer, and direct torque and flux control with space vector modulation (DTFC-SVM) for the interior permanent magnet synchronous motor (IPMSM), without signal injection. The concept of "active flux" (or "torque producing flux") turns all the rotor salient-pole ac machines into fully nonsalient-pole ones. A new function for L_q inductance depending on torque is introduced to model the magnetic saturation. Notable simplification in the rotor position and speed estimation is obtained, because the active flux position is identical with the rotor position. Extensive experimental results are presented to verify the principles and to demonstrate the effectiveness of the proposed sensorless control system. With the active flux observer, the IPMSM drive system operates from very low speed of 2 r/min at half full-load up to 1400 r/min. Higher speed is possible, in principle, with flux weakening.**

***Index Terms*—Flux observers, permanent magnet synchronous motors, sensorless control, state estimation, torque control, variable speed drives.**

I. Introduction

In THE last few years, various motion-sensorless control algorithms based on signal-injection magnetic saliency, even processing of certain pulsewidth modulation voltage sequences, involving low, even zero, speed, have been proposed for interior permanent magnet synchronous motors (IPMSMs) [1]–[17]. An initial position estimation sequence is added [15]–[17].

For very low-speed (3–10 r/min) servo drives, the inherent signal injection algorithms complexity is to be accepted. The low-speed operation is quite critical by using electromotive force (EMF) techniques for the rotor position estimation based on fundamental model [18]–[23], without signal injection. At very low speed, the stator voltage is very small, and thus, flux or rotor position estimations become very difficult to obtain. Moreover, at low speed, flux and position observers are very sensitive to machine parameter variations, especially to the stator resistance that varies with temperature [21].

However, the motion-sensorless control of ac drives based on fundamental-model state observers is aiming at lower and lower speeds. At these low speeds (below 10 r/min, in general), the voltage drop on the inverter power devices has to be taken into consideration at low frequency (low-voltage amplitude) because it becomes comparable with the stator fundamental voltage itself, and thus, distortions and discontinuities in voltage waveforms occur [14]. All very low-speed, flux and position observers must be provided with a compensator of inverter nonlinearities and with techniques for online estimation of the stator resistance [21].

A simplified rotor flux observer based on fundamental combined voltage–current model with PM flux–amplitude correction loop and simple dc d-axis current injection is shown in [23] to "survive" even at zero speed for surface PMSM drives.

A very recent fundamental model based on the "active flux" theoretical concept (elimination of rotor saliency) is developed in [22] for all ac machines, and proven by digital simulations only for the IPMSM case. This concept is considered as an extension (generalization) to all ac machines of the "extended EMF" [19]–[21] and the "fictitious PM flux" [24] concepts. The magnetic cross-coupling saturation effects are easier to account because an equivalent rotor nonsalient-pole ac machine model is introduced. The active flux position is identical to the rotor position, fact that greatly simplifies the rotor position and speed estimation at all speeds, in an effort to reduce online computation effort.

The main claims of this paper lay into the active-flux-based state observer implementation and DTFC-SVM sensorless control for IPMSM drives, with extensive experimental tests to provide very low-speed operation without any signal injection. A new function for the inductance L_q depending on torque is introduced to model the magnetic saturation.

The proposed sensorless control system has been verified experimentally, and has been proven to work from very low operating speed (2 r/min) at half rated load, up to 1400 r/min, with good estimation accuracy both in speed transients and steady state. The proposed method is intended to general ac drives that allow a little hesitation at start and do not require sustained operation under 2 r/min.

II. Active Flux Concept

The "active flux" concept [22] turns all rotor salient-pole ac machines into fictitious rotor nonsalient-pole machines such that the rotor position and speed estimations become simpler. For self-sufficiency, the active flux expression will be derived here in short.

The active flux $\overline{\psi}_d^a$ is defined as the flux that multiplies the i_q current component in the dq-model torque (T_e) expression of

Manuscript received March 21, 2008; revised June 14, 2008. Current version published May 19, 2009. This work was supported in part by the Ministry of Education and Research, Romania, under Grant CEEX X2C33/2006. Paper no. TEC-00104-2008.

I. Boldea and M. C. Paicu are with the Department of Electrical Engineering, University Politehnica of Timisoara, Timisoara 300223, Romania (e-mail: boldea@lselinux.upt.ro; paicucodruta@yahoo.com).

G.-D. Andreescu is with the Department of Automation and Applied Informatics, University Politehnica of Timisoara, Timisoara 300223, Romania (e-mail: daniel.andreescu@aut.upt.ro).

F. Blaabjerg is with the Institute of Energy Technology, Aalborg University, Aalborg 9220, Denmark (e-mail: fbl@iet.aau.dk).

Digital Object Identifier 10.1109/TEC.2009.2016137

all ac machines in rotor reference frame. For the IPMSM

$$T_e = 1.5 p_1 \psi_d^a i_q \tag{1}$$

with

$$\psi_d^a = \psi_{\rm PM} + (L_d - L_q)\, i_d, \qquad L_d < L_q \tag{2}$$

where p_1 is the number of pole pairs, L_d and L_q are the *dq* inductances, $\psi_{\rm PM}$ is the PM flux linkage, and the d-axis corresponds to the rotor pole (PM) axis.

$\overline{\psi}_d^a$ has the d-axis orientation (2). This means that the active flux position is identical to the rotor position in any operation mode, leading to a great simplification in rather accurate rotor position and speed estimation whenever active flux estimation is feasible.

$\overline{\psi}_d^a$ represents the total torque producing flux (1), including the reluctance torque component (2). Thus, the IPMSM model (3) in rotor reference frame (without superscript) "looses" the magnetic anisotropy and manifests itself by the inductance L_q

$$\overline{V}_s = R_s \bar{i}_s + (s + j\omega_r) L_q \bar{i}_s + (s + j\omega_r)\overline{\psi}_d^a \tag{3}$$

$$\overline{\psi}_d^a = \overline{\psi}_s - L_q \bar{i}_s \tag{4}$$

where $\overline{V}_s$, $\bar{i}_s$, and $\overline{\psi}_s$ are the stator voltage, current, and flux vectors; R_s is the stator resistance; and ω_r is the electrical rotor speed. The derivation of (3) is straightforward (see Appendix).

The simplicity of (4) *in any reference frame* looks striking, but it is just natural. Note that, if the stator flux $\overline{\psi}_s$ is estimated in stator reference frame, then the active flux estimation is straightforward, with magnetic saturation influence present in L_q that greatly simplifies its accountancy in the model.

The *dq* components of the model (3) become

$$\begin{bmatrix} V_d \\ V_q \end{bmatrix} = \begin{bmatrix} R_s + sL_q & -\omega_r L_q \\ \omega_r L_q & R_s + sL_q \end{bmatrix} \begin{bmatrix} i_d \\ i_q \end{bmatrix} + \begin{bmatrix} s\psi_d^a \\ \omega_r \psi_d^a \end{bmatrix}. \tag{5}$$

To explicit the concept quickly, the steady-state vector diagram with $\overline{\psi}_d^a$ in foreground is drawn in Fig. 1.

The stator voltage model in stator coordinates is

$$\overline{V}_s^s = R_s \bar{i}_s^s + \frac{d\overline{\psi}_s^s}{dt}. \tag{6}$$

The active flux observer $\overline{\psi}_d^{as}$ is derived from (4) and (6) in stator coordinates

$$\overline{\psi}_d^{as} = \int (\overline{V}_s^s - R_s \bar{i}_s^s + \overline{V}_{\rm comp})dt - L_q \bar{i}_s^s \tag{7}$$

where $\overline{\psi}_d^{as}$ axis falls along the rotor d-axis, and thus

$$\overline{\psi}_d^{as} = \psi_d^a \cos\theta_{\psi_d^a} + j\psi_d^a \sin\theta_{\psi_d^a}. \tag{8}$$

$\overline{V}_{\rm comp}$ is the total compensating vector in the integrator from (7) for various errors in $\overline{\psi}_s$ estimation as: integrator dc-offset, integrator initial condition, stator resistance, and inverter nonlinearities (power switch voltage drops, dead time).

The active flux observer (7) is practically the same in structure for all ac machines. It leads to the estimation of both ψ_d^a amplitude and $\theta_{\psi_d^a}$ angle with respect to stator phase a. Note that for PMSMs, $\theta_{\psi_d^a} = \theta_{\rm er}$, i.e., electrical rotor position. To provide decoupled torque control, ψ_d^a may be kept rather constant up to based speed.

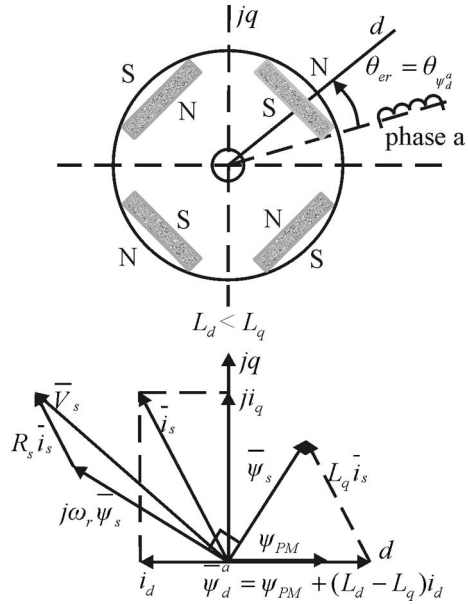

Fig. 1. IPMSM and its vector diagram pointing out the active flux $\overline{\psi}_d^a$.

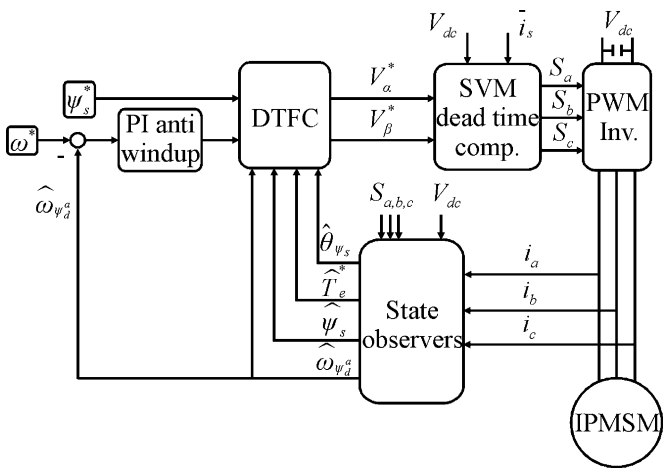

Fig. 2. Proposed DTFC-SVM sensorless control system for IPMSM.

III. DTFC-SVM Sensorless Control System

Fig. 2 illustrates the proposed DTFC-SVM sensorless control system for IPMSM, which contains: the speed controller, the DTFC-SVM control, the active-flux-based state observer with rotor position and speed estimator, and the torque estimator. The DTFC-SVM system uses the voltage model (6) in stator flux reference, and ensures decoupled control of flux and torque, and fast torque responses.

The DTFC scheme, shown in Fig. 3, involves two parallel closed loops with PI controllers operating in stator flux reference frame: the torque control loop with $(T_e^*, \hat{T}_e)$ pair and the stator flux magnitude control loop with $(\psi_s, \hat{\psi}_s)$ pair.

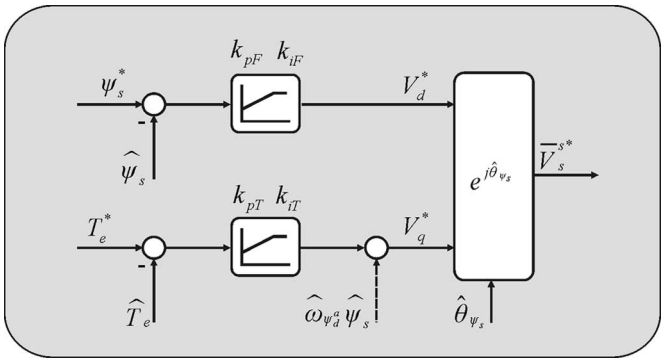

Fig. 3. DTFC structure in stator flux reference frame.

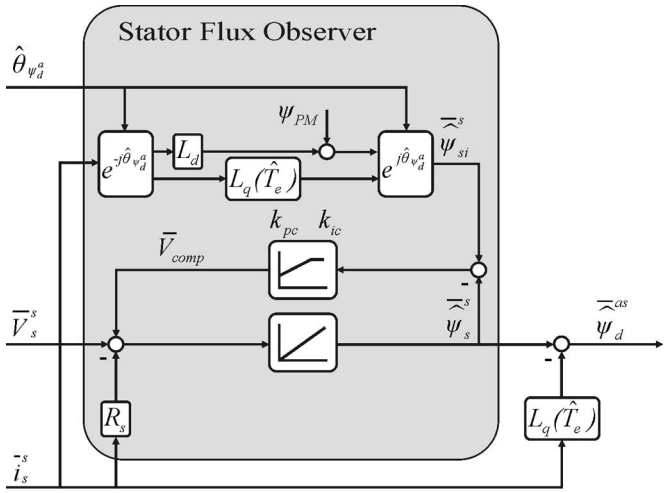

Fig. 4. Active flux observer with $L_q(\hat{T}_e)$ (9).

They provide the stator voltage reference in stationary reference frame ($\overline{V}_s^{s*}$) by using the estimated stator flux angle ($\hat{\theta}_{\psi s}$) in the rotator operator.

DTFC method has been proven more robust in sensorless control since it does not use Park operator, typical in vector control; thus, the estimated position error is not important [25].

The voltage-source inverter (VSI) switching signals (S_a, S_b, and S_c) are generated by the space vector modulation (SVM) block, which employs the dead time and inverter nonlinearities compensations [14] to realize a suitable stator voltage vector reference. This way, the torque and current pulsations are significantly reduced. This compensation is indispensable for accurate active flux estimation, especially at very low speed.

For IPMSM with the data given in Table I (see Appendix), using trial and error procedure, the proportional and integral gains for the PI controller on the d-axis are $k_{pF} = 10$ and $k_{iF} = 10\ \mathrm{s}^{-1}$, and for the PI controller on the q-axis are $k_{pT} = 3$ and $k_{iT} = 30\ \mathrm{s}^{-1}$. The PI controllers have the form: $k_p(1 + k_i/s)$.

The speed controller is also of PI type with antiwindup and torque limiter, and with a first-order low-pass filter on speed reference ω_r^*. The PI gains are $k_{pw} = 0.1$ and $k_{iw} = 10\ \mathrm{s}^{-1}$.

IV. State Observers

A. Active Flux Observer

The main purpose of the active flux observer is to estimate the active flux vector using the measured stator current and the estimated stator voltage. The stator voltage is estimated from the measured dc voltage V_{dc} and the inverter switching states.

The active flux observer implementation scheme is shown in Fig. 4, and consists of a stator flux observer $\overline{\hat{\psi}}_s^s$ in large speed range based on the combined voltage–current model, from which the term $L_q\bar{i}_s^s$ is subtracted (7).

The stator flux observer combines advantages of the current-model estimator in rotor reference at low speed, with the voltage-model estimator in stator reference at medium–high speed, employing a PI compensator that decides the flux estimation dynamic behavior in frequency domain [13].

At very low speed, including zero speed ($\omega_e \to 0$), the PI compensator gain, characterized in frequency domain by $k_{\mathrm{pc}} - jk_{ic}/\omega_e$, has very high value. Thus, the stator flux estimation $\overline{\hat{\psi}}_s^s$ follows the stator flux reference given by the open-loop current model $\overline{\hat{\psi}}_{si}^s$ to reduce the flux error.

At medium–high speed, the PI compensator gain practically remains only with the proportional component (low k_{pc}), and now, the correction loop could be considered an open one. Thus, the stator flux estimation $\overline{\hat{\psi}}_s^s$ is given only by the voltage model. The dc-offset ($\omega_e = 0$) from the measured current and voltage chains is totally compensated.

In conclusion, the frequency behavior of the PI compensator provides for the stator flux estimation a smooth transition, depending on speed, between the open-loop current model—sensitive to magnetic parameter variations (ψ_{PM}, L_d, and L_q), and the closed-loop voltage model—with mildly R_s influence.

The PI compensator gains are tuned by pole allocation method choosing double pole at 2 rad/s, resulting $k_{\mathrm{pc}} = 4$ and $k_{ic} = 4$. $R_s = 4\ \Omega$ is set for hot-temperature value.

Finally, the magnetic saturation with mild cross-coupling effect for IPMSM is considered by the new function $L_q(\hat{T}_e)$

$$L_q = L_{qn}/(1 + k_T|\hat{T}_e|/T_{en}) \tag{9}$$

where L_{qn} is the L_q nominal value, k_T is a torque coefficient (for our case, $k_T = 0.2$), $\hat{T}_e$ is the estimated torque, and T_{en} is the rated torque value.

The current model in the stator flux observer (Fig. 4) employs the same $L_q(\hat{T}_e)$ function (9). The L_d inductance is constant (the permanent magnets are in the d-axis), and the cross-coupling effect is rather small as the currents do not exceed 150% rated value to limit the inverter ratings and costs, as usual in industrial drives. Fig. 5 illustrates by digital simulations the influence of the magnetic saturation of L_q (9) in the active flux observer, for full step load response at 2 r/min with and without considering the saturation. In simulation, the machine model always includes the magnetic saturation according to (9).

It is evident that the estimated speed from the active flux observer with considered saturation is much closer to the actual

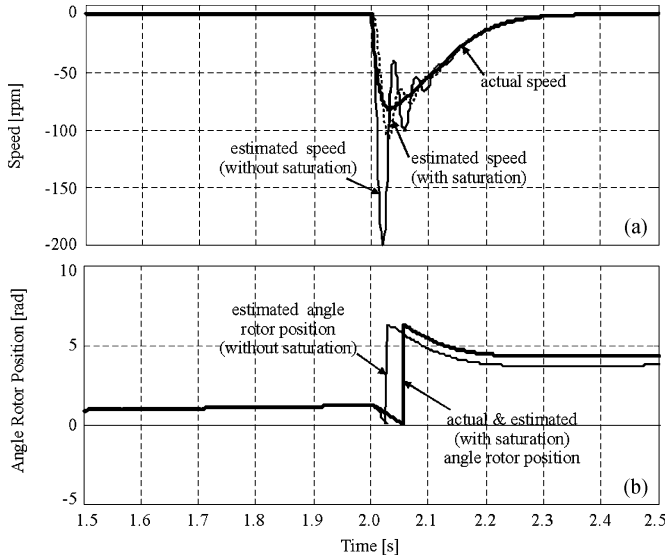

Fig. 5. Influence of L_q magnetic saturation in the active flux observer for sensorless operation at lowest speed of 2 r/min (0.1 Hz) and step of 100% rated torque. (a) Actual speed, estimated speed with saturation, and estimated speed without saturation. (b) Actual rotor position, estimated rotor position with saturation, and estimated rotor position without saturation—simulation results.

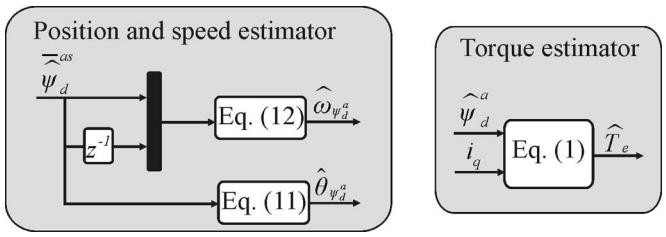

Fig. 6. Position–speed estimator and torque estimator.

speed; also, the estimated rotor position is much closer to the actual rotor position.

B. Position–Speed Estimator and Torque Estimator

The rotor position–speed estimator and torque estimator implementation is illustrated in Fig. 6. As the active flux vector falls along the rotor d-axis, its speed is identical to the rotor speed, which greatly simplifies the speed estimation.

To extract the rotor position and speed from the active flux vector, a solution is to use a phase-locked loop (PLL) state observer. Another solution applied here is to employ derivative estimator based on (10)–(12)

$$\hat{\omega}_{\psi_d^a} = \frac{d\hat{\theta}_{\psi_d^a}}{dt} \tag{10}$$

$$\hat{\theta}_{\psi_d^a} = a\tan\left(\frac{\hat{\psi}_{d\beta}^a}{\hat{\psi}_{d\alpha}^a}\right) \tag{11}$$

$$\hat{\omega}_{\psi_d^a} = \frac{\hat{\psi}_{d\alpha k-1}^a \hat{\psi}_{d\beta k}^a - \hat{\psi}_{d\beta k-1}^a \hat{\psi}_{d\alpha k}^a}{h(\hat{\psi}_{d\alpha k}^{a2} + \hat{\psi}_{d\beta k}^{a2})} \tag{12}$$

where h is the sampling time and the index k-1 in (12) denotes variables delayed with one sampling period.

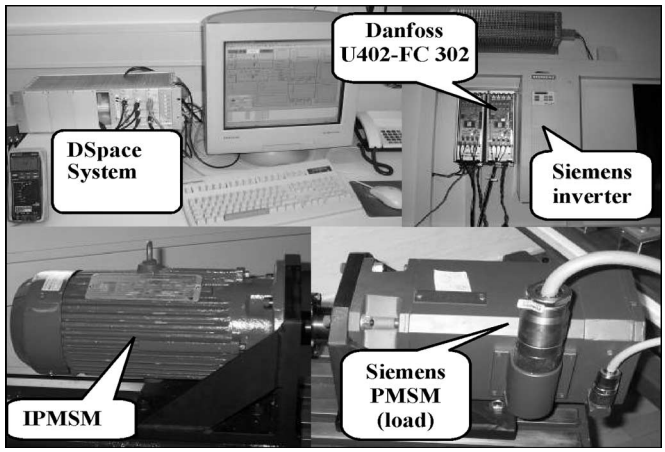

Fig. 7. Experimental setup of the proposed sensorless DTFC-SVM system.

A low-pass filter (LPF) (13) is applied to the estimated speed to reduce noise, where $k_{pF} = 1$ and $T_{iF} = 0.003$ s

$$H_{LPF} = \frac{k_{pF}}{(T_{iF}s + 1)}. \tag{13}$$

If the active flux vector is correctly estimated, the electromagnetic torque $\hat{T}_e$ is simply computed based on (1).

From the active flux observer, the rotor position estimation is used in rotator operators in Fig. 4, and the rotor speed estimation is used for the speed control loop.

None of them are used in DTFC-SVM (Fig. 3), this fact being an inherent advantage of DTFC motion-sensorless control.

V. Experimental Platform and Test Results

The proposed sensorless direct torque and flux control (DTFC-SVM) is validated on the experimental prototype with the data presented in Table I (see Appendix).

Fig. 7 illustrates a three-phase 2.2-kW IPMSM directly coupled to the load machine (Siemens PMSM), which is speed-controlled by a frequency inverter (Siemens Simovert Masterdrive). A three-phase IGBT inverter, supplied at a dc-link voltage of 540 V, feeds the IPMSM. The sampling frequency and PWM frequency are set to 10 kHz. The inverter dead time is set to 2 μs. Phase currents are measured using magnetic current transducers. The actual rotor position and speed are provided by an incremental encoder with 2048 pulses per revolution, only for comparison.

All the experimental tests have been carried out with a limited value (50%) of the rated motor torque because we did not have a stable loading machine at very low speed for more than 50% rated torque.

The design and simulation of the sensorless control system is realized in MATLAB/Simulink, and is implemented on a DSpace PPC 1103 real-time controller board.

Experimentally, it is observed that the control is sensitive to dead time compensation (the stator voltage applied to machine is lower than the stator voltage reference because of dead time losses), and to the stator resistance, especially at low speeds.

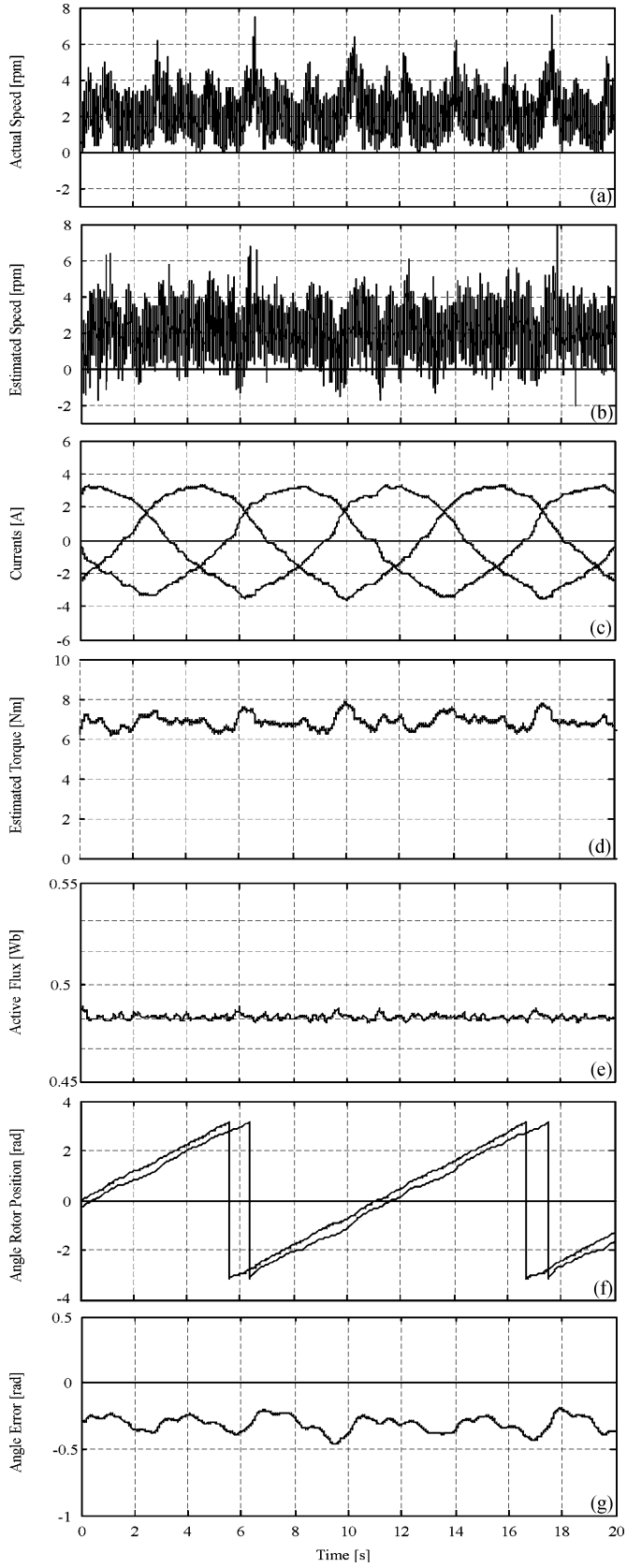

Fig. 8. Steady-state sensorless operation at lowest speed of 2 r/min (0.1 Hz) and 50% rated torque. (a) Actual speed. (b) Estimated speed. (c) Measured currents. (d) Estimated torque. (e) Active flux. (f) Rotor position (actual and estimated). (g) Error between estimated and actual rotor position.

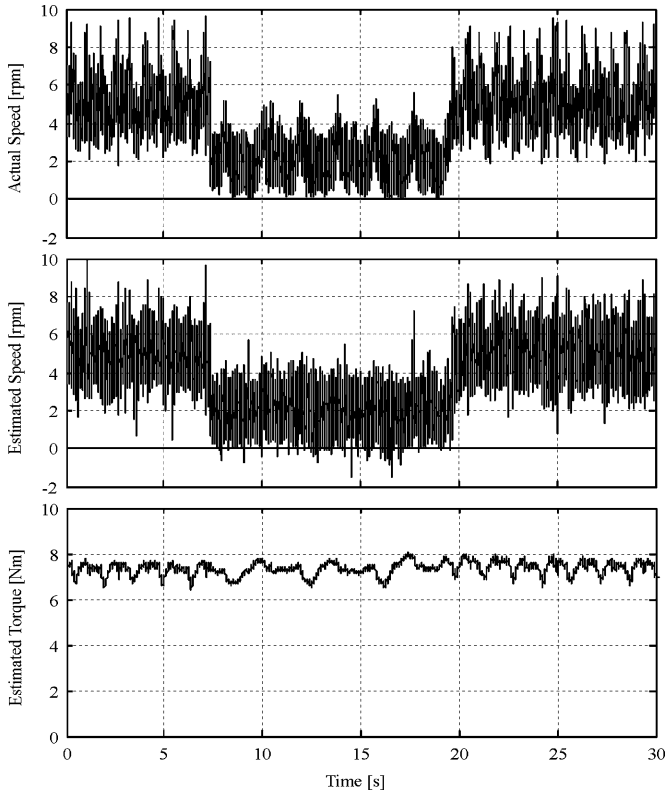

Fig. 9. Transients from 5 (0.25 Hz) to 2 r/min (0.1 Hz) at 50% rated torque. (a) Actual speed. (b) Estimated speed. (c) Estimated torque.

The start-up procedure is mandatory, and it aligns the rotor at zero by triggering a proper set of voltage vectors ($\overline{V}_1(1,0,0)$).

The following experimental tests are performed to check the concepts and performance of the proposed motion-sensorless control system:

1) steady-state operation at lowest speed (2 r/min) and 50% rated torque (Fig. 8);
2) step speed reduction from 5 to 2 r/min at 50% rated torque (Fig. 9);
3) ± 10 r/min speed reversal at 50% rated torque (Fig. 10);
4) step torque response at 20 r/min (Fig. 11);
5) start-up response from zero to 1400 r/min, followed by ± 1400 r/min speed reversal, plus 50% step torque loading response (Figs. 12 and 13).

The experimental results for sensorless operation at the lowest speed limit of 2 r/min and 50% rated torque are acceptable (see Fig. 8), taking into account that the novel concept of active flux is applied, and not signal injection methods. Even with partial compensation of the VSI nonlinearities, the currents and the torque are not quite smooth, and the measured speed has some pulsations but in acceptable limits for general variable-speed drive applications. These speed pulsations could be due to the cogging torque, partial-compensated inverter nonlinearities, and other nonmodeled disturbances.

To check the dynamics at very low speeds, operation from 5 to 2 r/min, is tested with good results (Fig. 9).

Fig. 10 shows the results obtained from a speed reversal operation at ± 10 r/min and 50% of rated torque. Here, the currents

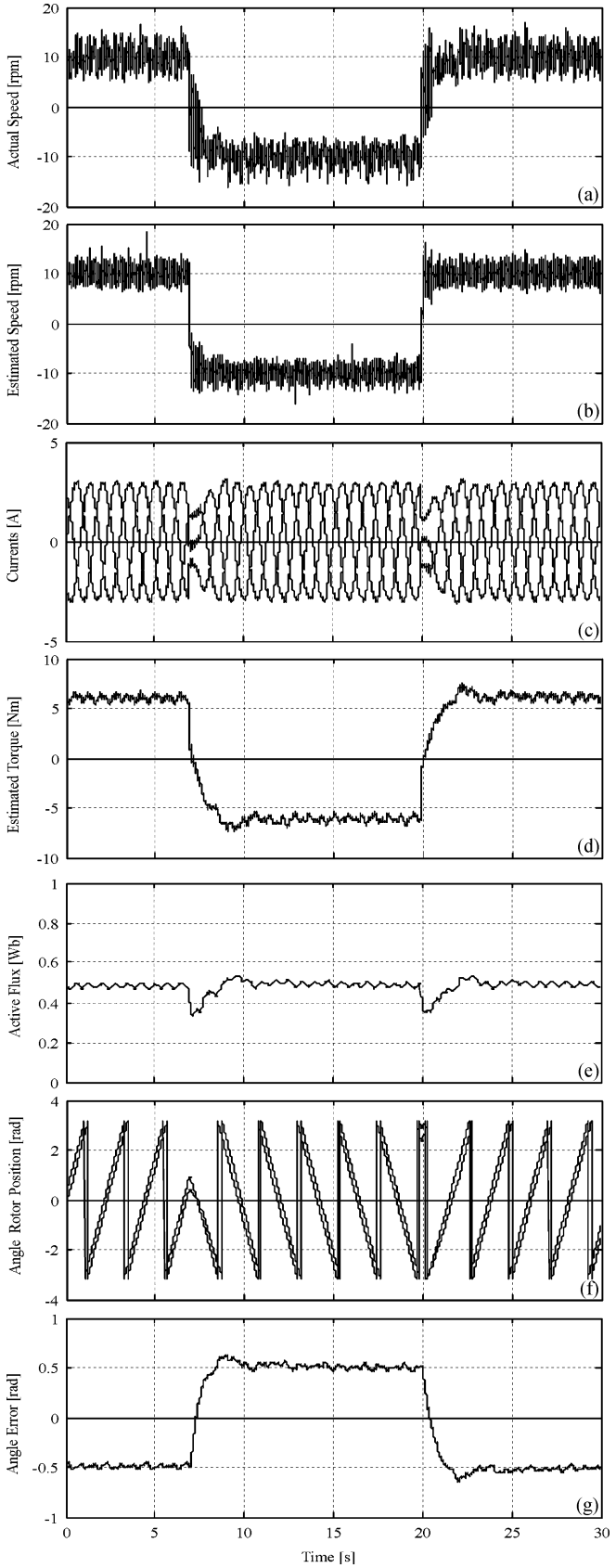

Fig. 10. Speed reversal at ± 10 r/min (0.5 Hz) and 50% rated torque. (a) Actual speed. (b) Estimated speed. (c) Measured currents. (d) Estimated torque. (e) Active flux. (f) Rotor position (actual and estimated). (g) Error between estimated and actual rotor position.

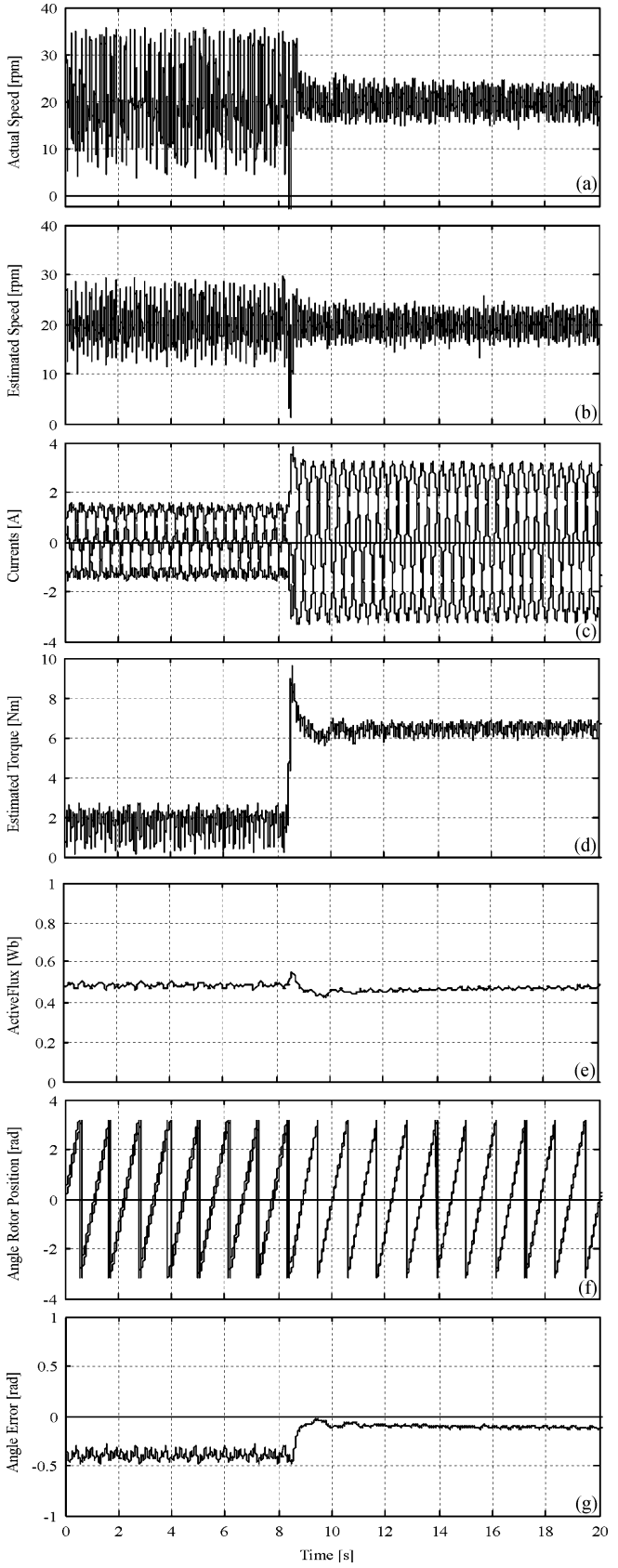

Fig. 11. Torque transients at 20 r/min (1 Hz) and 50% rated torque. (a) Actual speed. (b) Estimated speed. (c) Measured currents. (d) Estimated torque. (e) Active flux. (f) Rotor position (actual and estimated). (g) Error between estimated and angle rotor position.

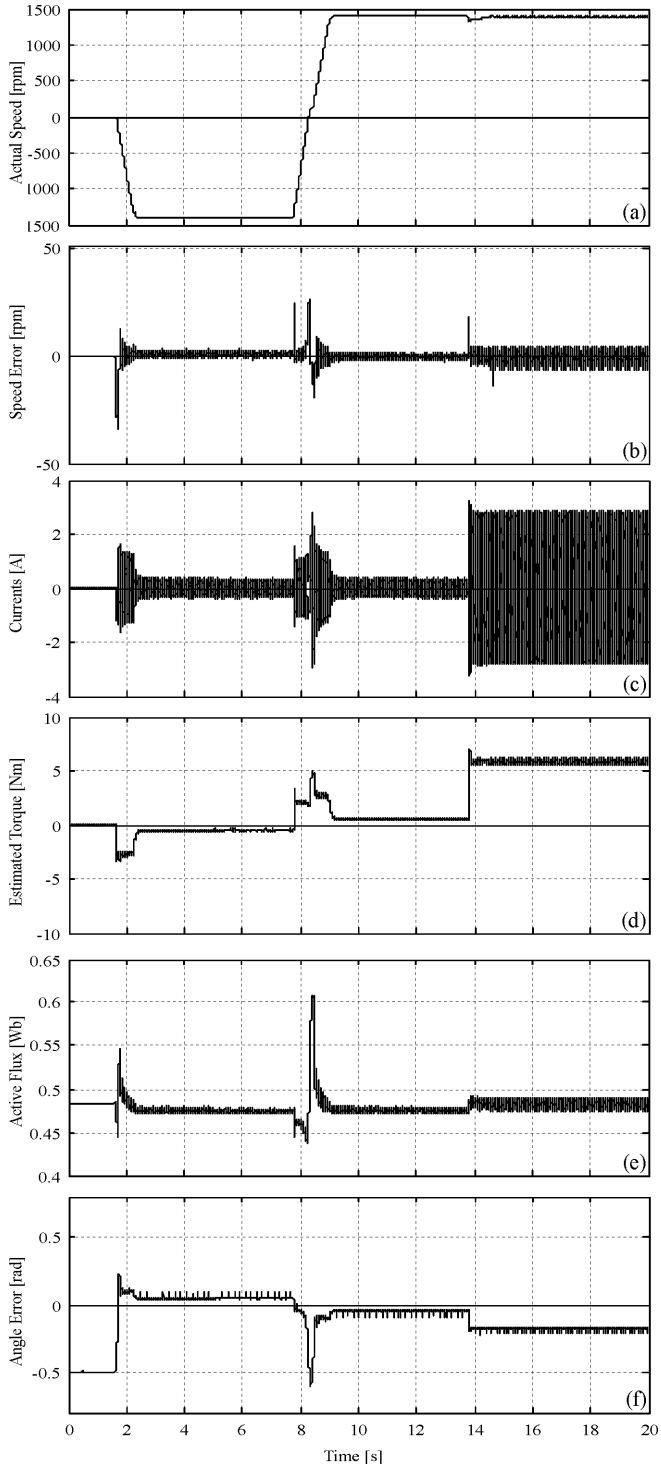

Fig. 12. Start-up response from 0 to -1400 r/min (70 Hz), speed reversal at ∓ 1400 r/min and torque transients at 1400 r/min at 50% rated torque. (a) Actual speed. (b) Error between estimated and actual speed. (c) Measured currents. (d) Estimated torque. (e) Active flux. (f) Error between estimated and actual rotor position.

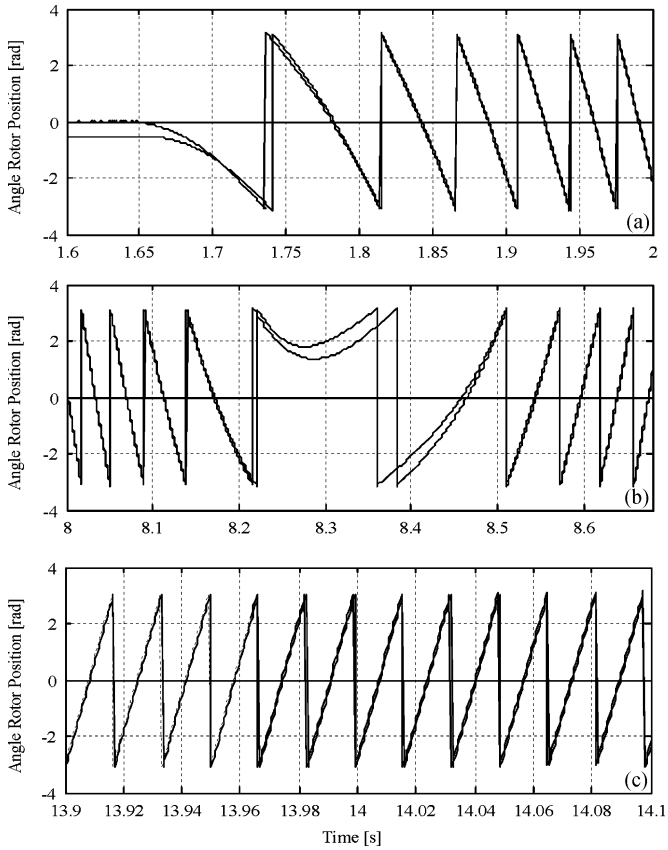

Fig. 13. Start-up response from 0 to -1400 r/min (70 Hz), speed reversal at ∓ 1400 r/min and torque transients at 1400 r/min at 50% of nominal torque. Zoom for actual rotor position at (a) start-up, (b) speed reversal, (c) step torque load.

are smooth, the torque shows some pulsations, but they are again reasonable.

Torque transients at 20 r/min for step-loading from 0% to 50% rated torque, with an acceptable overshooting are presented in Fig. 11.

The rotor position errors in Figs. 8, 10, and 11 are visible, but limited to reasonable values. Note that if the rotor position error is constant, then the speed estimation will be correct.

In all tests, during torque transients, the stator flux is kept constant (Fig. 3), while the active flux could vary.

Since in DTFC, the rotor position estimation enters only in the stator flux current model, which is important only at low speeds, the position error at medium and high speeds is not important at all.

The speed estimation error really counts because a speed feedback is used for speed loop control. The speed estimation errors are up to 30 r/min during speed transients, but they go down to less than 2–5 r/min during steady state.

Start-up response from 0 to -1400 r/min, speed reversal at ∓ 1400 r/min, and torque transients at 1400 r/min at 50% rated torque are all shown in Figs. 12 and 13 with good expected dynamics at high speeds.

VI. Conclusion

A novel-state observer for flux, rotor position, and speed in wide speed range (2–1400 r/min) is developed and implemented based on the active flux concept particularized for IPMSM drive. No signal injection is involved. The magnetic saturation is modeled by a new function for L_q inductance depending on torque.

TABLE I
IPMSM SPECIFICATIONS

Rated power	2.2 kW
Rated speed	1750 rpm
Rated frequency	87.5 Hz
Rated torque	12 Nm
Rated phase to phase voltage	380 V (rms)
Rated phase current	4.1 A (rms)
Number of pole pairs (p_1)	3
Stator resistance per phase (R_s)	3.3 Ω
d-axis inductance (L_d)	41.6 mH
q-axis inductance (L_q)	57.1 mH
Permanent magnet flux ($\_{PM}$)	0.483 Vs/rad
Total inertia (J)	$10.1\text{x}10^{-3}$ kgm^2
Viscous friction coefficient (B)	$20\text{x}10^{-4}$ Nm s/rad
Windings connection	star connection

A motion-sensorless control system for IPMSM drive with DTFC-SVM using the proposed observer is investigated by extensive significant experimental tests with good results.

Through experimental tests, sustained sensorless operation at low speed down to 2 r/min is obtained, with stable operation to 50% rated load torque. The rotor position errors are visible, but limited. They occur, however, only in the active flux observer at very low speeds because DTFC is performed.

Flux weakening for torque–speed envelope strong extension may be performed as usual with IPMSM.

The proposed solution is a general approach that can be used in motion-sensorless control of universal ac drives.

APPENDIX

Let us start with the *dq*-model of IPMSM in rotor reference frame, where we add and subtract new terms (the last parenthesis) in both equations

$$V_d = R_s i_d + sL_d i_d - \omega_r L_q i_q + (sL_q i_d - sL_q i_d) \quad \text{(A1)}$$

$$V_q = R_s i_q + sL_q i_q + \omega_r(\psi_{\mathrm{PM}} + L_d i_d) + (\omega_r L_q i_d - \omega_r L_q i_d). \quad \text{(A2)}$$

Adding the two equations to prepare them for space phasor form

$$V_d + jV_q = R_s(i_d + ji_q) + sL_q(i_d + ji_q) + j\omega_r L_q(i_d + ji_q) + s(\psi_{\mathrm{PM}} + (L_d - L_q)i_d) + j\omega_r(\psi_{\mathrm{PM}} + (L_d - L_q)i_d) \quad \text{(A3)}$$

with $\psi_d^a = \psi_{\mathrm{PM}} + (L_d - L_q)i_d$, finally leads to

$$\overline{V}_s = R_s\bar{i}_s + (s + j\omega_r)L_q\bar{i}_s + (s + j\omega_r)\psi_d^a. \quad \text{(A4)}$$

Evidencing distinctly the transformer and motion-induced voltages by L_q in the *dq*-model (A_4) is a definitive sign that the active flux IPMSM machine is now a pure nonsalient-pole rotor model, both for steady state and transients.

REFERENCES

[1] M. W. Degner and R. D. Lorenz, "Using multiple saliencies for the estimation of flux, position and velocity in AC machines," *IEEE Trans. Ind. Appl.*, vol. 34, no. 5, pp. 1097–1104, Sep./Oct. 1998.

[2] F. Briz, M. W. Degner, P. Garcia, and R. D. Lorenz, "Comparison of saliency-based sensorless control techniques for AC machines," *IEEE Trans. Ind. Appl.*, vol. 40, no. 4, pp. 1107–1115, Jul./Aug. 2004.

[3] M. Linke, R. Kennel, and J. Holtz, "Sensorless speed and position control of synchronous machines using alternating carrier injection," in *Proc. IEEE-IEMDC 2003*, Jun., vol. 2, pp. 1211–1217.

[4] A. Consoli, G. Scarcella, and A. Testa, "Industry application of zero-speed sensorless control techniques for PM synchronous motors," *IEEE Trans. Ind. Appl.*, vol. 37, no. 2, pp. 513–521, Mar./Apr. 2001.

[5] C. Silva, G. M. Asher, and M. Sumner, "Hybrid rotor position observer for wide speed-range sensorless PM motor drives including zero speed," *IEEE Trans. Ind. Electron.*, vol. 53, no. 2, pp. 373–378, Apr. 2006.

[6] S. Shinnaka, "New "mirror-phase vector control" for sensorless drive of permanent-magnet synchronous motor with pole saliency," *IEEE Trans. Ind. Appl.*, vol. 40, no. 2, pp. 599–606, Mar./Apr. 2004.

[7] P. L. Jansen and R. D. Lorenz, "Transducerless position and velocity estimation in induction and salient AC machines," *IEEE Trans. Ind. Appl.*, vol. 31, no. 2, pp. 240–247, Mar./Apr. 1995.

[8] N. Bianchi and S. Bolognani, "Influence of rotor geometry of an IPM motor on sensorless control feasibility," *IEEE Trans. Ind. Appl.*, vol. 43, no. 1, pp. 87–96, Jan./Feb. 2007.

[9] E. Robeischl and M. Schroedl, "Optimized INFORM measurement sequence for sensorless PM synchronous motor drives with respect to minimum current distortion," *IEEE Trans. Ind. Appl.*, vol. 40, no. 2, pp. 591–598, Mar./Apr. 2004.

[10] P. Guglielmi, M. Pastorelli, G. Pellegrino, and A. Vagati, "Position-sensorless control of permanent-magnet-assisted synchronous reluctance motor," *IEEE Trans. Ind. Appl.*, vol. 40, no. 2, pp. 615–622, Mar./Apr. 2004.

[11] M. F. Rahman, L. Zhong, Md. E. Haque, and M. A. Rahman, "A direct torque-controlled interior permanent-magnet synchronous motor drive without a speed sensor," *IEEE Trans. Energy Convers.*, vol. 18, no. 1, pp. 17–22, Mar. 2003.

[12] I. Boldea, C. I. Pitic, C. Lascu, G.-D. Andreescu, L. Tutelea, F. Blaabjerg, and P. Sandholdt, "DTFC-SVM motion-sensorless control of PM-assisted reluctance synchronous machine as starter-alternator for hybrid electric vehicles," *IEEE Trans. Power Electron.*, vol. 21, no. 3, pp. 711–719, May 2006.

[13] G.-D. Andreescu, C. I. Pitic, F. Blaabjerg, and I. Boldea, "Combined flux observer with signal injection enhancement for wide speed range sensorless direct torque control of IPMSM drives," *IEEE Trans. Energy Convers.*, vol. 23, no. 2, pp. 393–402, Jun. 2008.

[14] J. Holtz and J. Quan, "Drift- and parameter-compensated flux estimator for persistent zero-stator-frequency operation of sensorless-controlled induction motors," *IEEE Trans. Ind. Appl.*, vol. 39, no. 4, pp. 1052–1060, Jul./Aug. 2003.

[15] H. Kim, K.-K. Huh, R. D. Lorenz, and T. M. Jahns, "A novel method for initial rotor position estimation for IPM synchronous machine drives," *IEEE Trans. Ind. Appl.*, vol. 40, no. 5, pp. 1369–1378, Sep./Oct. 2004.

[16] Y. Jeong, R. D. Lorenz, T. M. Jahns, and S. Sul, "Initial rotor position estimation of an interior permanent magnet synchronous machine using carrier-frequency injection methods," in *Proc. IEEE-IEMDC-2003*, Jun., vol. 2, pp. 1218–1223.

[17] J. Holtz, "Initial rotor polarity detection and sensorless control of PM synchronous machines," in *Proc. Conf. Rec. IEEE-IAS 2006*, Oct., vol. 4, pp. 2040–2047.

[18] H. Kim, M. C. Harke, and R. D. Lorenz, "Sensorless control of interior permanent-magnet machine drives with zero-phase lag position estimation," *IEEE Trans. Ind. Appl.*, vol. 39, no. 6, pp. 1726–1733, Nov./Dec. 2003.

[19] Z. Chen, M. Tomita, S. Ichikawa, S. Doki, and S. Okuma, "Sensorless control of interior permanent magnet synchronous motor by estimation of an extended electromotive force," in *Proc. Conf. Rec. IEEE-IAS 2000*, Oct., vol. 3, pp. 1814–1819.

[20] S. Morimoto, K. Kawamoto, M. Sanada, and Y. Takeda, "Sensorless control strategy for salient-pole PMSM based on extended EMF in rotating reference frame," *IEEE Trans. Ind. Appl.*, vol. 38, no. 4, pp. 1054–1061, Jul./Aug. 2002.

[21] S. Morimoto, M. Sanada, and Y. Takeda, "Mechanical sensorless drives of IPMSM with online parameter identification," *IEEE Trans. Ind. Appl.*, vol. 42, no. 5, pp. 1241–1248, Sep./Oct. 2006.
[22] I. Boldea, M. C. Paicu, and G.-D. Andreescu, "Active flux concept for motion sensorless unified AC drives," *IEEE Trans. Power Electron.*, vol. 23, no. 5, pp. 2612–2618, Sep. 2008.
[23] E. Urlep and K. Jezernik, "Low and zero speed sensorless control of nonsalient PMSM," in *Proc. Conf. Rec. IEEE-ISIE 2007*, Jun., pp. 2238–2243.
[24] S. Koonlaboon and S. Sangwongwanich, "Sensorless control of interior permanent-magnet synchronous motors based on a fictitious permanent-magnet flux model," in *Proc. Conf. Rec. IEEE-IAS 2005*, Oct., vol. 1, pp. 311–318.
[25] M. P. Kazmierkowski, R. Krishnan, and F. Blaabjerg, *Control in Power Electronics: Selected Problems*. London, U.K.: Academic, 2002, ch. 9.

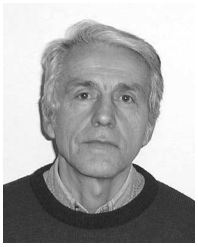

Ion Boldea (M'77–SM'81–F'96) received the M.S. and Ph.D. degrees from the University Politehnica of Timisoara, Timisoara, Romania, in 1967 and 1973, respectively.

He is currently a Full Professor in the University Politehnica of Timisoara. He has visited universities in the U.S. and the U.K. repeatedly, and has published extensively on linear and rotary electric machines, drives, and power electronics. He has authored or coauthored books (with S. A. Nasar): *Electric Drives* (2^{nd} Edition) (Boca Raton: CRC Press, 2005), *The Induction Machine Handbook* (Boca Raton: CRC Press, 2001), and *The Electric Generator Handbook* (parts 1 and 2) (Boca Raton: CRC Taylor & Francis, 2005). He is an Associate Editor of the *Electric Power Components and Systems* and the Director of the Internet-only *Journal of Electric Engineering* (www.jee.ro).

Prof. Boldea is a member of the Industrial Drives and the Electric Machines Committees of the IEEE Industry Applications Society (IAS). He was the Chairman of the OPTIM International Conferences (IEEE-IAS sponsored) in 1996, 1998, 2000, 2002, 2004, 2006, and 2008.

Mihaela Codruta Paicu was born in Gorj, Romania, in 1981. She received the B.E. degree in electrical engineering in 2005 from the University Politehnica of Timisoara, Timisoara, Romania, where she is currently working toward the Ph.D. degree in the Department of Electric Drives and Power Electronics.

Her current research interests include testing and control of interior permanent magnet synchronous motors.

Gheorghe-Daniel Andreescu (M'03–SM'05) was born in Caracal, Olt, Romania, on March 17, 1953. He received the Diplom.-Eng. (M.S.) degree in applied electronics and the Ph.D. degree in automatic control systems from the University Politehnica of Timisoara, Timisoara, Romania, in 1977 and 1999, respectively.

From 1994 to 2002, he was engaged in automatic testing for avionics, e.g., at British Airways Avionic Eng. (BAAE), Cardiff, U.K. He is currently a Full Professor in the Department of Automation and Applied Informatics, University Politehnica of Timisoara. He has authored or coauthored over 50 papers published in journals and international conferences and two books. His current research interests include advanced control of ac drives— sensorless control, observers, sliding-mode control, mechatronic systems—robotics, automatic testing for avionics, microcontroller and very high speed integrated circuit hardware description language (VHDL) applications, monitoring and control of distributed systems.

Prof. Andreescu is a member of the IEEE Industrial Applications Society and the IEEE Robotics and Automation Society, the International Federation of Automatic Control (IFAC) Technical Committee on Mechatronic Systems, the Romanian Society of Control Engineering and Technical Informatics, and the Expert Evaluators Group within the Engineering Science Commission of the National University Research Council, Romania.

Frede Blaabjerg (S'86–M'88–SM'97–F'03) was born in Erslev, Denmark, on May 6, 1963. He received the M.Sc.E.E. and Ph.D. degrees from the Institute of Energy Technology, Aalborg University, Aalborg, Denmark, in 1987 and 1995, respectively.

From 1987 to 1988, he was with ABB-Scandia, Randers, Denmark. In 1992, he was an Assistant Professor at Aalborg University, where he became an Associate Professor in 1996, a Full Professor in power electronics and drives in 1998, and is currently the Dean of the Faculty of Engineering, Science and Medicine. In 2000, he was a Visiting Professor in the University of Padova, Padova, Italy, as well as a part-time Programme Research Leader in wind turbines at the Research Center, Risoe. In 2002, he was a Visiting Professor at Curtin University of Technology, Perth, Australia. He has been involved in many research projects within the industry. Among them is the Danfoss Professor Programme in power electronics and drives. He has authored or coauthored more than 500 publications in his research fields including *Control in Power Electronics* (New York: Academic, 2002). He is an Associate Editor for the *Journal of Power Electronics* and *Elteknik*. He has been involved in Danish Research Policy for the last ten years. His current research interests include power electronics, static power converters, ac drives, switched reluctance drives, modeling, characterization of power semiconductor devices and simulation, wind turbines, and green power inverters.

Prof. Blaabjerg is the Editor-in-Chief of the IEEE TRANSACTIONS ON POWER ELECTRONICS. He is a member of the Danish Academy of Technical Science, the European Power Electronics and Drives Association, and the IEEE Industry Applications Society. From 2005 to 2007, he was a Distinguished Lecturer for the IEEE Power Electronics Society . He has received the 1995 Angelos Award for his contribution in modulation technique and control of electric drives, the Annual Teacher Prize from Aalborg University in 1995, the Outstanding Young Power Electronics Engineer Award from the IEEE Power Electronics Society in 1998, eight IEEE Prize paper awards, the C. Y. O'Connor Fellowship from Perth, Australia, in 2002, the Statoil Prize for his contributions in power electronics in 2003, and the Grundfos Prize for his contributions in power electronics and drives in 2004.